# Liposomal delivery of a Pin1 inhibitor complexed with cyclodextrins as new therapy for high-grade serous ovarian cancer

Concetta Russo Spena[a,b], Lucia De Stefano[a,b], Stefano Palazzolo[a], Barbara Salis[c,d], Carlotta Granchi[e], Filippo Minutolo[e], Tiziano Tuccinardi[e], Roberto Fratamico[f], Sara Crotti[g], Sara D'Aronco[g,h], Marco Agostini[g,h], Giuseppe Corona[i], Isabella Caligiuri[d], Vincenzo Canzonieri[d], Flavio Rizzolio[a,j,*]

[a] *Department of Translational Research, Experimental and Clinical Pharmacology, Center for Molecular Biomedicine – CRO, National Cancer Institute, Aviano, Italy*
[b] *Doctoral School in Chemistry, University of Trieste, Italy*
[c] *Doctoral School in Molecular Biomedicine, University of Trieste, Italy*
[d] *Department of Molecular Biology and Translational Research, Pathology Unit, Center for Molecular Biomedicine – CRO, National Cancer Institute, Aviano, Italy*
[e] *Department of Pharmacy, University of Pisa, Italy*
[f] *Department of Medical Oncology, Sidney Kimmel Cancer Center, Thomas Jefferson University, Philadelphia, PA, USA*
[g] *Città della Speranza, Institute of Pediatric Research, Padova, Italy*
[h] *Department of Surgical, Oncological and Gastroenterological Sciences, First Surgical Clinic Section, University of Padova, Italy*
[i] *Department of Molecular Biology and Translational Research, Immunopathology and Cancer Biomarkers Unit, Center for Molecular Biomedicine – CRO, National Cancer Institute, Aviano, Italy*
[j] *Department of Molecular Sciences and Nanosystems, Ca' Foscari University, Venezia-Mestre, Italy*

ARTICLE INFO

*Keywords:*
Pin1
Ovarian cancer
Liposome
Inhibitory small molecules

ABSTRACT

Pin1, a prolyl isomerase that sustains tumor progression, is overexpressed in different types of malignancies. Functional inactivation of Pin1 restrains tumor growth and leaves normal cells unaffected making it an ideal pharmaceutical target. Although many studies on Pin1 have focused on malignancies that are influenced by sex hormones, studies in ovarian cancer have lagged behind. Here, we show that Pin1 is an important therapeutic target in high-grade serous epithelial ovarian cancer. Knock down of Pin1 in ovarian cancer cell lines induces apoptosis and restrains tumor growth in a syngeneic mouse model. Since specific and non-covalent Pin1 inhibitors are still limited, the first liposomal formulation of a Pin1 inhibitor was designed. The drug was efficiently encapsulated in modified cyclodextrins and remotely loaded into pegylated liposomes. This liposomal formulation accumulates preferentially in the tumor and has a desirable pharmacokinetic profile. The liposomal inhibitor was able to alter Pin1 cancer driving-pathways trough the induction of proteasome-dependent degradation of Pin1 and was found to be effective in curbing ovarian tumor growth *in vivo*.

## 1. Introduction

High-grade serous epithelial ovarian cancer (HGSOC) is a deadly disease, which accounts for > 150.000 deaths each year worldwide [1]. For decades, treatment strategies for HGSOC have shown little improvement in overall survival and the use of cytoreductive surgery followed by platinum-based chemotherapy remains the first-line treatment [1–3]. Although most patients respond to platinum based therapy, the majority relapse and die from the disease [4–9]. Lack of knowledge regarding tumor origin has been the major limitation in the discovery of new therapeutic agents. Only recently, new mouse models have clarified that secretory epithelial cells of the distal fallopian tube (FTSECs) are the likely progenitors of a substantial proportion of HGSOCs [10–14]. In addition, progress in the molecular characterization of tumors derived directly from patients have defined important pathways for the development and progression of HGSOCs [15,16]. Alterations of homologous recombination, PI3K/RAS, RB, NOTCH, and FOXM1 pathways are commonly found [15].

A fundamental mechanism in controlling key proteins in these pathways is the phosphorylation of the proline (Pro)-Ser/Thr motifs, which are controlled by the Peptidyl-prolyl *cis-trans* isomerase NIMA-interacting 1 (Pin1), a unique Peptidyl-prolyl isomerase (PPIase) [17,18]. Pin1 accelerates the conversion of *cis* and *trans* isomers, which is slowed down by phosphorylation. The net result is the activation of

* Corresponding author at: Department of Molecular Sciences and Nanosystems, Ca' Foscari University, Venezia-Mestre, Italy.
*E-mail address:* flavio.rizzolio@unive.it (F. Rizzolio).

Accepted 30 April 2018

oncogenes and inactivation of tumor suppressor genes in cancer cells [19–27]; therefore, its inhibition represents an exciting therapeutic target for the treatment of HGSOCs. In addition, Pin1 possesses other unique features which are attractive as a therapeutic target: a) the PPIase domain has a specific, structurally-organized shaped active site that is suitable for drug development [28]; b) mice knocked down (KD) for Pin1 are viable without gross abnormalities [29] and c) genetic manipulation of Pin1 in several oncogene-induced mouse models of tumorigenesis limits tumor burden and metastatic spread [30]. Pin1 is expressed at low levels in normal tissues and specifically upregulated in cancer cells and cancer stem cells, a subclass of neoplastic cells found in most tumors which are more resistant to commonly used chemotherapy drugs [31]. Furthermore, inhibition of Pin1 sensitizes cancer cells to targeted- and chemo-therapies and reverses drug resistance [32,33]. Many research groups and companies are developing Pin1 ligands; however, in spite of highly specific molecular inhibition, they lack demonstrated effective inhibition of Pin1 and antitumor activity in vivo [34]. In turn, no clinical trials have been performed due to inadequate pharmacological parameters of developed inhibitors such as potency, solubility, and cell permeability [35]. Only recently, it has been discovered a specific Pin1 inhibitor possessing an in vivo activity, albeit with a covalent mechanism of action [36].

A current approach in improving pharmacokinetic (PK) parameters and toxicity profile of drugs is the development of nanoparticles for drug delivery [37]. Nanodrugs have many fundamental properties that are necessary in cancer therapy: specific accumulation in the tumor taking advantage of enhanced permeability and retention (EPR) effect [38], increased therapeutic ratio (high effectiveness and low toxicity) and improved drug solubility. Although thousands of nanomaterials are under investigation, liposomes, a bilayer of lipids that mimic the cell membrane are of great interest [39–41].Other than biocompatibility, these nanomaterials have already been approved by the Food and Drug Administration in the United States and the European Medicines Agency in Europe [42–45].

Here we demonstrated that Pin1 is overexpressed in ovarian cancer tissue samples and when knocked down, promotes ovarian cancer cell death in vitro and in vivo demonstrating its potential as pharmacological cancer target for HGSOC. For the first time, we encapsulated a selective Pin1 inhibitor (compound 17 in Guo et al.,) designed by Pfizer into liposomes. This small molecule is among the most potent Pin1 inhibitors but with low solubility and poor permeability [34]. Utilizing a similar method developed by Vogelstein's group [46], we successfully loaded the drug/modified cyclodextrin complex by remote loading into liposomes and utilized it to kill ovarian cancer cells in an *in vivo* model.

## 2. Experimental section

### 2.1. Materials

#### 2.1.1. Liposomal formulation

1,2-distearoyl-*sn*-glycero-3-phosphocholine **(**DSPC), cholesterol, 1,2- dipalmitoyl-*sn*-glycero-3-phosphoethanolamine-N-[methoxy(polyethylene glycol)-2000] **(**DPPE-PEG), polycarbonate membranes from Avanti Polar Lipids (Alabaster, AL, US). Heptakis-(6-amino-6-deoxy)-β-Cyclodextrin 7xHCl, CDexB-013 from Arachem (Netherlands). Slide-A-Lyzer® MINI Dialysis Devices, 20 K MWCO from ThermoFisher Scientific (Waltham, MA, US). Instrumentation: DLS Zetasizer Nano ZSP (ZEN 5600) from Malvern Instruments (United Kingdom). NanoDrop 2000c from ThermoFisher Scientific (Waltham, MA, US).

#### 2.1.2. In vitro experiments

*2.1.2.1. Tissue microarrays*. OV2001 and OV802 from US Biomax Inc. (Rockville, MD, US). Antibody rabbit PIN1 1:50 (sc-15340) from Santa Cruz (Santa Cruz, CA, US). Instrumentation: Benchmark ultra instrument from Ventana Medical Systems (Tucson, AZ, US).

*2.1.2.2. Cell cultures*. OVCAR3, MRC-5, T47D, PLC/PRF/5 and NIH-3T3 cell lines from ATCC (Manassas, VA, US). Kuramochi and COV318 cell lines were generously provided by Gustavo Baldassarre. STOSE cell line was generously provided by Barbara Vanderhyden.

*2.1.2.3. shRNA*. Human Pin1 KD1 (TRCN0000001033), KD2 (TRCN0000010577) and mouse Pin1 KD1 (TRCN0000012580), KD2 (TRCN0000012582) from Sigma-Aldrich Merck (Germany).

*2.1.2.4. Oligonucleotides*. m/h Pin1-f: 5-CAAGGAGGAGGCCCTGGAGC; m/h Pin1-r: 5-TGCA TCTGACCTCTGCTGAAGG;m HPRT-f: 5-AGTACTTCAGGGATTTGAATCACG; m HPRT-r: 5- GGACTC CTCGTATTTGCAGATTC; βact-Fw: 5-GACCCAGATCATGTTTGAGA; βact-rev: GACTCCATGCCCAGGAAG from IDT Technology (Coralville, IA, US).

*2.1.2.5. Flow cytometry analysis*. Propidium iodide and RNase A from Roche (Switzerland). PE-Annexin V Apoptosis Detection Kit from Becton-Dickinson (Franklin Lakes, NJ, US). Instrumentation and software: for sub G1 analysis, FACscan instrument from Becton-Dickinson (Franklin Lakes, NJ, US) and ModFit LTV4.0.5 (Win) software; for Annexin V analysis, FACS Canto II from Becton-Dickinson (Franklin Lakes, NJ, US) and BD FACS DIVA software.

*2.1.2.6. Cell viability and caspase 3/7 assays*. CellTiter-Glo®luminescent cell viability assay and caspase 3/7 Glo assay from Promega (Madison, WI, US). NP-40 lysis buffer: 0.01 M Tris-HCl, 0.01 M NaCl, 0.003 M $MgCl_2$, 0.03 M sucrose, and 0.5% NP-40. Instrumentation: F200 Tecan instrument from Tecan (Switzerland). The $IC_{50}$ was calculated using the GraphPad program from Prism (La Jolla, CA, US).

*2.1.2.7. RNA analysis*. Smarter Nucleic Acid Sample Preparation kit from Stratec biomedical (Germany). Go-Script RT System kit and GoTaq® G2 Polymerase and Master Mix from Promega (Madison, WI, US).

*2.1.2.8. Western blot analysis*. Phosphatase inhibitors (Complete-EDTA free) from Roche (Switzerland). TruePage Precast Gels 4–12% SDS-PAGE from Sigma-Aldrich Merck (Germany). Amersham TM Protran TM 0.45 μm NC from GE Healthcare Life Science (Pittsburgh, PA, US). RIPA buffer: 10 mM Tris-Cl (pH 8.0), 1% NP-40, 0.1% sodium deoxycholate, 0.1% SDS, 140 mM NaCl. Antibodies: mouse Cyclin D1 1:1000 (556470) from BD Pharmigen™ (Franklin Lakes, NJ, US); rabbit β-catenin 1:1000 (#8480S), rabbit β-actin 1:1000 (#4967S) and rabbit HA-tag (#3724S) from Cell Signaling Technology (Danvers, MA, US); rabbit LC3B 1:1000 (GTX127375) from GeneTex (Irvine, CA, US); rabbit Pin1 1:250 (sc-15340), mouse Pin1 1:250 (sc-46660) and mouse Hsp70 1:1000 (sc-24) from Santa Cruz (Santa Cruz, CA, US); rabbit α-tubulin 1:2000 (T9026) from Sigma-Aldrich Merck (Germany). Secondary antibodies anti-rabbit (31464, 1:5000) and anti-mouse (31432, 1:5000) from ThermoFisher Scientific (Waltham, MA, US). Software: Image J (NIH).

#### 2.1.3. In vivo experiments

Liquid chromatography tandem mass spectrometry (LC-MS/MS): Ultra-grade acetonitrile and formic acid (> 98%) from Romil LTD (United Kingdom). Instrumentation: Qiagen Tissue Ruptor from Qiagen (Germantown, MD, US). UltiMate 3000 system from ThermoFisher Scientific, (Waltham, MA, US) coupled to an API 4000 triple quadrupole mass spectrometer from AB SCIEX (Framingham, MA, US) working

in multiple reaction monitoring (MRM) modality. Hypersil GOLD C8 column 2.1 × 100 mm, 3 µm, from ThermoFisher Scientific (Waltham, MA, US). Milli-Q Academic/Quantum EX system from Millipore (Milford, MA, US).

*2.1.3.1. Biodistribution, PK and Tumor growth*. 8 week-old female FVB/N mice and 6 week-old female athymic nude FOXN1$^{NU}$ mice from Envigo (United Kingdom). Cultrex® Basement Membrane Matriz, Type 3 from Trevigen (Gaithersburg, MD, US).

### 2.2. Methods

#### 2.2.1. Liposomal formulation

A representative Pin1 inhibitor (compound 8, Scheme S1; compound 17 in Guo et al. [34],), belonging to the alkyl amide indole-based library of compounds developed by Pfizer was synthesized in our laboratory following the previously reported procedure [34] (see Supplemental methods).

*2.2.1.1. Pegylated liposomes*. DSPC, cholesterol and DPPE-PEG (50:45:5, molar ratio) were dissolved in chloroform (20 mL). The solvent was removed by vacuum to form a thin lipid film, which was hydrated by shaking in the appropriate buffer (80 mM Arg·Hepes, pH 9) at 65 °C for 2 h. The vesicle suspension was serially extruded through 0.4-, 0.2- and 0.1-µm polycarbonate membranes, 10 times for each membrane, at 65 °C to obtain mono-dispersed liposomes. The transmembrane gradient was then created by dialyzing liposomes overnight in PBS. The average size and polydispersity index were measured by dynamic light scattering experiments.

Cyclodextrin-Inhibitor (CI) complex: compound 8 was dissolved in methanol and mixed with equimolar quantity of Heptakis-(6-amino-6-deoxy)-β-Cyclodextrin 7xHCl in deionized water. In detail, the methanolic solution of the drug was added in a dropwise fashion to the cyclodextrin solution in agitation (final concentration of methanol was 10%). This suspension was shaken at 55 °C for 48 h. The solution was flash-frozen in a dry ice/acetone bath followed by lyophilization and then stored at −20 °C until further use.

*2.2.1.2. Liposomes/cyclodextrin/compound 8 (LC8) complex*. After lyophilization, CI was incubated with 20 mg/mL of liposomal solution for 1 h at 65 °C. The sample was spun at 13.8 ×*g* for 5 s in order to remove the particulate matter. The amount of compound 8 loaded within the liposomes was determined by UV-VIS method utilizing a calibration curve. The compound 8 and LC8 were dissolved in methanol and analyzed at 270 nm.

The loading efficiency of compound 8 was evaluated after disruption of the liposomal solution with methanol: 5 µL of LC8 was dissolved in 600 µL of methanol. The rate of release of compound 8 from the liposomes was evaluated using a dialysis membrane at 37 °C in PBS 1 ×. It was utilized 1 mg/mL of compound 8 in the LC8 formulation.

#### 2.2.2. In vitro experiments

*2.2.2.1. Immunohistochemical analysis*. Human ovarian carcinoma and normal ovarian tissue microarrays were incubated with Pin1 antibody for 1 h at room temperature utilizing the ultraview DAB detection kit with CC1 buffer for 36 min in Benchmark ultra instrument.

The ovarian tissues were analyzed with light microscopy using 10 and 20× magnifications. The immunohistochemical (IHC) staining was converted to an H score: intensity (0, 1, 2, 3) × area (0–100%). The H score from 0 to 75 (first quartile) was defined as low expression and > 75 was defined as medium-high expression. Two pathologists scored IHC staining independently.

All mouse tissues were fixed for 24 h in formalin and embedded in paraffin. Each slide was 3 µm thick, counterstained with hematoxylin/eosin and analyzed at 20/40× of magnification. IHC of Pin1 was done using the same criteria as human tissues.

*2.2.2.2. Flow cytometry, caspase 3/7 and cell viability analyses*. OVCAR3, MRC-5, T47D, PLC/PRF/5 and NIH3T3 cell line grown as indicated by supplier. Kuramochi and COV318 cell line grown in RPMI and DMEM media with 10% FBS, respectively. STOSE cell line grown in DMEM media with 4% FBS. Pin1 knock down experiments were performed as previously described [23]. Briefly polyclonal populations of transduced cells were generated by infection with 1 MOI (multiplicity of infectious units) of shRNA lentiviral particles.

*2.2.2.2.1. Sub G1 analysis*. Cells were fixed by adding ice-cold 70% ethanol while vortexing. Fixed cells were stored at 4 °C for at least 2 h and then washed once with PBS. Cells were stained with 1 µg/mL propidium iodide, 500 ng/mL RNase A in PBS and incubated at room temperature for 1 h in the dark. Sub G1 analysis was performed after 5 days.

Annexin V analysis was performed according to the manufacturer's protocol. Cells were stained with PE Annexin V and 7-AAD and incubated for 30 min at room temperature in the dark. 300 µL of 1× binding buffer were added to each tube. Samples were evaluated within 1 h. Annexin V analysis was performed after 5 days.

*2.2.2.2.2. Caspase 3/7 assay*. 1 × $10^5$ cells were lysed in 10 µL of NP-40 buffer and incubated with 10 µL of caspase 3/7 kit for 1 h at room temperature. Caspase 3/7 assay was done after 3 days.

*2.2.2.2.3. Cell viability*. The cells were infected with three different plasmids: two knock down and a control. Three days after infection the cells were seeded in 96-well plates at a density of $10^3$ cells/well. The viability was evaluated by luminescent assay. Averages and standard deviations were obtained from triplicates.

*2.2.2.3. RT-PCR, real-time PCR and western blot analyses*

*2.2.2.3.1. Reverse transcription*. 400 ng of total RNA were prepared from cells using the Smarter Nucleic Acid Preparation kit and were reverse transcribed in a 10 µL reaction using Go-Script RT System kit. 4 ng of cDNA were used to amplify target genes.

*2.2.2.3.2. Semi-quantitative PCR*. cDNA was amplified using GoTaq® G2 Polymerase and Master Mix. Hprt was used as a control. PCR reactions were carried out in a final volume of 20 µL as described in the manufacturer's protocol. The PCR cycles were as follow: 5 min at 95 °C; 20 s at 95 °C, 30 s at 60 °C, 30 s at 72 °C × 30 cycles. The products were analyzed via 3% agarose gel electrophoresis.

*2.2.2.3.3. Western blot analysis*. Total cell extracts were obtained by treating cells with RIPA buffer 0.1% SDS plus protease and phosphatase inhibitors then incubate on ice for 20 min and sonicated for 5 s. After centrifuging at 13.8 ×*g* for 20 min at 4 °C, equal amount of protein (50 µg) was separated by TruePage Precast Gels. Proteins were transferred onto nitrocellulose membranes, then blocked for 30 min with 5% non-fat dried milk in TBS containing 0.1% Tween 20 (TBS-T). The membranes were incubated with primary antibodies at 4 °C ON, washed three times with TBS-T and incubated with HRP-conjugated secondary antibodies for 1 h at room temperature. The results were visualized by ECL western blot analysis detection system.

*2.2.2.4. Half maximal inhibitory concentration ($IC_{50}$)*. In order to evaluate the $IC_{50}$ of compound 8 and LC8, cells were plated in a 96-well plate one day before treatment (OVCAR3: $10^3$ cells/well; MRC-5: $10^4$ cells/well). Then the cells were treated with LC8, cyclodextrin/compound 8, liposome/compound 8, compound 8 or empty liposomes starting with a concentration of 100 µM followed by five 1:2 serial

dilutions. After 96 h, the cell viability and $IC_{50}$ was evaluated by luminescent assay.

*2.2.2.4.1. Pin1 stability*. $3 \times 10^5$ NIH3T3 cells were plated one day before treatment. Cells were treated with 0, 50 and 100 μM of LC8, collected after 48 h and analyzed by RT-PCR or cells were treated with 100 μM of LC8 and DMSO as control for 24 h followed by 10 μg/mL of cycloheximide (CHX). Cells were collected after 0, 3, 6, 12 and 24 h for western blot analysis. Cells were also treated with 0, 50 and 100 μM of LC8 for 48 h and then treated with MG132 10 μM and after 6 h collected for western blot analysis.

*2.2.2.4.2. Pin1 target analysis*. T47D, PLC/PRF/5 and OVCAR3 were seeded with a density of $5 \times 10^5$ in 100 × 20 mm tissue culture dish one day before treatment. The cells were treated with 100 μM of compound 8 (LC8) and with 10 μM ATRA for 24 h and collected for western blot analysis.

### 2.2.3. In vivo experiments

*2.2.3.1. Animal studies*. Animal studies were done in accordance to the Italian Governing Law (D.lgs 26/2014) under the authorization of Ministry of Health n° 788/2015-PR and performed in accordance with the institutional guidelines. Data are reported as the mean and standard error.

*2.2.3.1.1. Immunocompetent tumor model*. $10^7$/1 mL STOSE cells were injected i.p. into 8 week-old female FVB/N mice.

*2.2.3.1.2. Immunodeficient tumor model*. $5 \times 10^6$ OVCAR3 cell line were mixed 1:1 with DMEM w/o phenol red/ Cultrex-Type 3 and implanted subcutaneously into the flank of 6 week-old female athymic nude $FOXN1^{NU}$ mice. When tumors reached the size of 168 ± 28 $mm^3$, mice were treated i.p. with LC8 one time per week for three treatments. Tumor volumes were measured with a caliper and calculated using the formula: (length × $width^2$)/2.

*2.2.3.1.3. PK*. The experiment was performed in 8 weeks-old FVB/N mice treated with 20 mg/kg (i.p.) of LC8 diluted in PBS 1×. 100 μL of blood were collected after 10 min, 3, 6, 12 and 24 h and analyzed by LC-MS/MS. A total of 200 μL were drawn from each mouse.

*2.2.3.1.4. Biodistribution*. Female nude mice were treated at a dose of 20 mg/kg of compound 8 (LC8) and sacrificed after 72 h. The organs were washed by perfusion with 10 mL of cold PBS/heparin before collection, diluted in 500 μL of PBS/BSA 4%, and homogenized with Qiagen Tissue Ruptor for 20 s at power 4 on ice.Samples were stored at −80 °C. The concentrations of inhibitor were measured by LC-MS/MS.

*2.2.3.2. LC-MS/MS*. Before extraction, a known amount of internal standard (IS) solution (Guo et al. [34], compound 16) was added to PK and biodistribution samples. Then, acetonitrile/0.1% formic acid was added (final volume ratio, 1:2). The samples were vortexed and placed into a sonicator bath for 5 min at 4 °C. This procedure was repeated twice and after centrifugation (13.8 ×*g*, 20 min, 4 °C), supernatants were collected together and dried under vacuum (Univapo 150H). Calculated extraction recoveries are reported in Table S1. Five-point calibration curves within the analyte concentration ranges 0.6–2857.1 ng/mL and 0.2–95 ng/mL were prepared in blank serum and tissue samples, obtained from untreated mice.

Selected transitions for Compound 8 and IS were as follows: *m/z* 423.1 > 206.1 and m/z 423.1 > 218.1 for Compound 8; *m/z* 391.1 > 206.2 and m/z 391.1 > 188.1 for IS. The optimized ESI (+) source parameters are reported in Table S1. Chromatographic separation was performed on a Hypersil GOLD C8 column. Elution was achieved by a linear gradient (mobile phase A: 0.1% formic acid, mobile phase B: acetonitrile/0.1% formic acid) from 30% to 95% B over 4 min. Injection volume was 10 μL and flow rate was 300 μL/min.

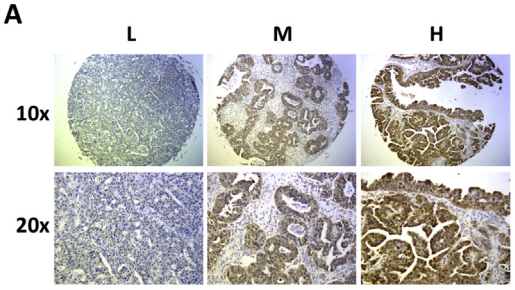


B

| | Pin1 | | |
|---|---|---|---|
| | Low | Mid-High | Total |
| Serous | **77** (42.8%) | **90** (50%) | **167** (92.8%) |
| Normal | **12** (6.7%) | **1** (0.5%) | **13** (7.2%) |
| Total | **89** (49.4%) | **91** (50.6%) | **180** (100%) |
| p_value | **0.0012** | | |

**Fig. 1.** Pin1 is highly expressed in HGSOC. (A) Representative images of Pin1 categorized as low (L), medium (M) and high (H) expression at different magnifications. (B) Pin1 protein is upregulated in cancer vs normal tissues. Fifty percent of cancer tissues have medium-high expression of Pin1 compared to 0.5% in normal tissues.

### 2.3. Statistical analysis

The statistical significance was determined using the two-tails paired *t*-test, unless specified. A $p$-value $< 0.05$ was considered significant for all comparisons done.

## 3. Results and discussion

### 3.1. Pin1 expression is altered in serous ovarian cancer patients

Pin1 controls many oncogenes and tumor suppressor genes and for this reason is of wide interest as a therapeutic target. Prior studies have focused on malignancies including breast and prostate cancer [47,48], however this is the first that deeply investigates Pin1 in ovarian cancer. As a first step, we took advantage of the whole genome data released from The Cancer Genome Atlas (TCGA) consortium. The data were filtered for the presence of multiple alterations (amplification, deletion and mutation) in different tumor types. Fig. S1 showed that Pin1 is mostly altered in hormonal cancers with HGSOC in the top position.

In support of the genomic amplification of Pin1, it has been reported to be frequently increased at the protein level in different types of cancers [49–54] and it is a good prognostic factor in hormone-dependent tumors [20,48]. A few analyses focused specifically on ovarian cancer [55]. To strength these data, we have analyzed by IHC 167 cases of serous ovarian cancer on tissue microarray (TMA). Among these, 59.4% were grade 3. The expression values were divided into two categories: low and medium-high (see Experimental section). In Fig. 1A, an example of these categories was reported. When compared to adjacent normal tissue (13 cases), Pin1 is significantly upregulated ($p$-value 0.0012, Fisher exact test) (Fig. 1B). Taking our data and the results from the TCGA into consideration, we concluded that Pin1 deserved further investigation as potential therapeutic target in ovarian cancer.

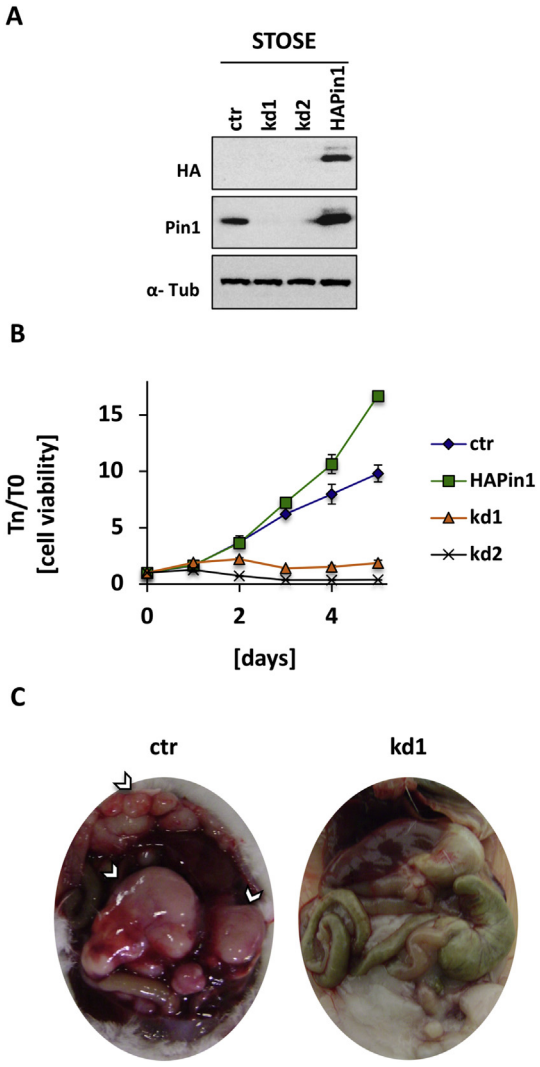


**Fig. 2.** Pin1 knock-down reduces tumor cell growth in vitro and shRNA treated cells implanted in vivo in a syngeneic model of HGSOC. (A) Western blot analysis of Pin1 downregulation (kd) and upregulation (HaPin1) in STOSE cells. (B) Cell viability of STOSE cells (Pin1 wild type, kd and overexpress) were monitored for 5 days. Values on y-axis: ratio between luminescence values at day n (Tn) normalized to day 0 (T0).(C) Representative images of FVB/N mice injected i.p. with STOSE cells wild type or kd for Pin1 (n = 3).

### *3.2. Pin1 knock-down reduces tumor cell growth in vitro and shRNA treated cells implanted in vivo in a syngeneic model of HGSOC*

To understand if Pin1 is a valid therapeutic target in HGSOC, we knocked down its expression in different ovarian cancer cell lines that recently have been demonstrated to closely represent ovarian cancer patients [56–58]. Firstly, Pin1 activity was evaluated in a spontaneously transformed mouse ovarian surface epithelial cancer cell line (STOSE), which strictly recapitulates the characteristics of human HGSOC [59]. Fig. 2A shows that mouse shRNAs efficiently down regulate the expression of Pin1. Pin1 knock down (KD) cells were less viable than normal cells and its upregulation increases cell viability (two side *t*-test, *p*-value $< 0.05$), (Fig. 2B). Since STOSE cell lines derived from FVB/N mice (syngeneic), normal and knock down cells were injected intraperitoneally (i.p.). Fig. 2C demonstrates that Pin1 KD abolishes tumor formation after > 3 months of follow up.

### *3.3. Pin1 knock down induces cell death in human HGSOC cell lines*

In order to evaluate if Pin1 affects cell viability in human cells, Kuramochi, COV318, and OVCAR3 cell lines were KD (Fig. 3A) and followed for 6 days. Pin1 KD cells were less viable than control cells (Fig. 3B).

The population of sub-G1 cells was evaluated in the same human cell lines, which showed an increase in sub-G1 phase in Pin1 KD cells (two side *t*-test, *p*-value $< 0.05$), (Fig. 3C). To discriminate if a real apoptotic mechanism was activated, cells were analyzed for Annexin V staining. The knock down cells have an increased number of apoptotic cells (early and total apoptosis) compared to normal cells (two side t-test, *p*-value $< 0.05$), (Fig. 3D,E). To gain insight into the molecular mechanism that leads to apoptosis, caspase 3/7 were evaluated.The activity of these protease enzymes is increased in knock down cells (two side t-test, *p*-value $< 0.05$) (Fig. 3F).

In conclusion, the results obtained from human and mouse HGSOC models confirmed that Pin1 is a valid therapeutic target for HGSOC patients.

### *3.4. Liposomal/cyclodextrin/compound 8 (LC8) has desired pharmacological properties*

Liposomal nanoparticles have been successful utilized as treatments for different diseases [60]. The major advantages are biocompatibility and an improved therapeutic window [61]. Unfortunately, only weakly acidic or basic drugs could be stably incorporated inside the cores of liposomes [62]. Recently, the Vogelstein group demonstrated that a hydrophobic drug could be solubilized in physiologic buffers and remote loaded into liposomes by modified cyclodextrins that have the properties of weak bases or acids [46].

A representative Pin1 inhibitor (compound 8, scheme S1), belonging to the alkyl amide indole-based library of compounds developed by Pfizer, was synthesized in our laboratory since it was among the most potent inhibitors of the isolated enzyme, showing a *Ki* value of 75 nM. This compound could be easily synthesized but it has a low solubility in water and is ineffective in cancer cells [34,63,64]. Compound 8 was solubilized in Heptakis (6-amino-6-deoxy)-β-cyclodextrins and loaded into pegylated-liposomes (see Experimental section for details). Compound 8 has a solubility of 0.30 ± 0.05 mg/mL. When formulated as a liposomal/cyclodextrin complex (Fig. 4A), the solubility of the Pin1 inhibitor increased by about 6 times (1.82 ± 0.10 mg/mL) (Fig. 4B). The loading efficiency of LC8 evaluated by UV absorbance was of 91.2 ± 5.0% (expressed as loaded /total drug ratio) (Fig. 4C). The hydrodynamic size of liposomes under different temperatures was determined by DLS. The size increased from 25 to 37 °C and remained stable up to 65 °C (Fig. S2A). The measures pre and post loading showed a low polydispersity index with the size of liposomes that increase from 151.8 ± 0.10 nm (pre) to 177 ± 0.11 nm (post) (Fig. 4D). The ability of LC8 to retain compound 8 was then tested. Fig. 4E demonstrates that the release from a semipermeable membrane of LC8 was slower than inhibitor alone. The accumulation of compound 8 into the liposome and the slow release rate may contribute to the change in the in vivo pharmacological properties. As proof of concept, LC8 was tested on OVCAR3 cells. Although compound 8 has no activity, LC8 has an $IC_{50}$ value in the low micromolar range (Fig. 4F and Fig. S2B). LC8 has no activity on MRC-5 normal fibroblasts (data not shown). These results allowed us to test LC8 in an in vivo mouse model.

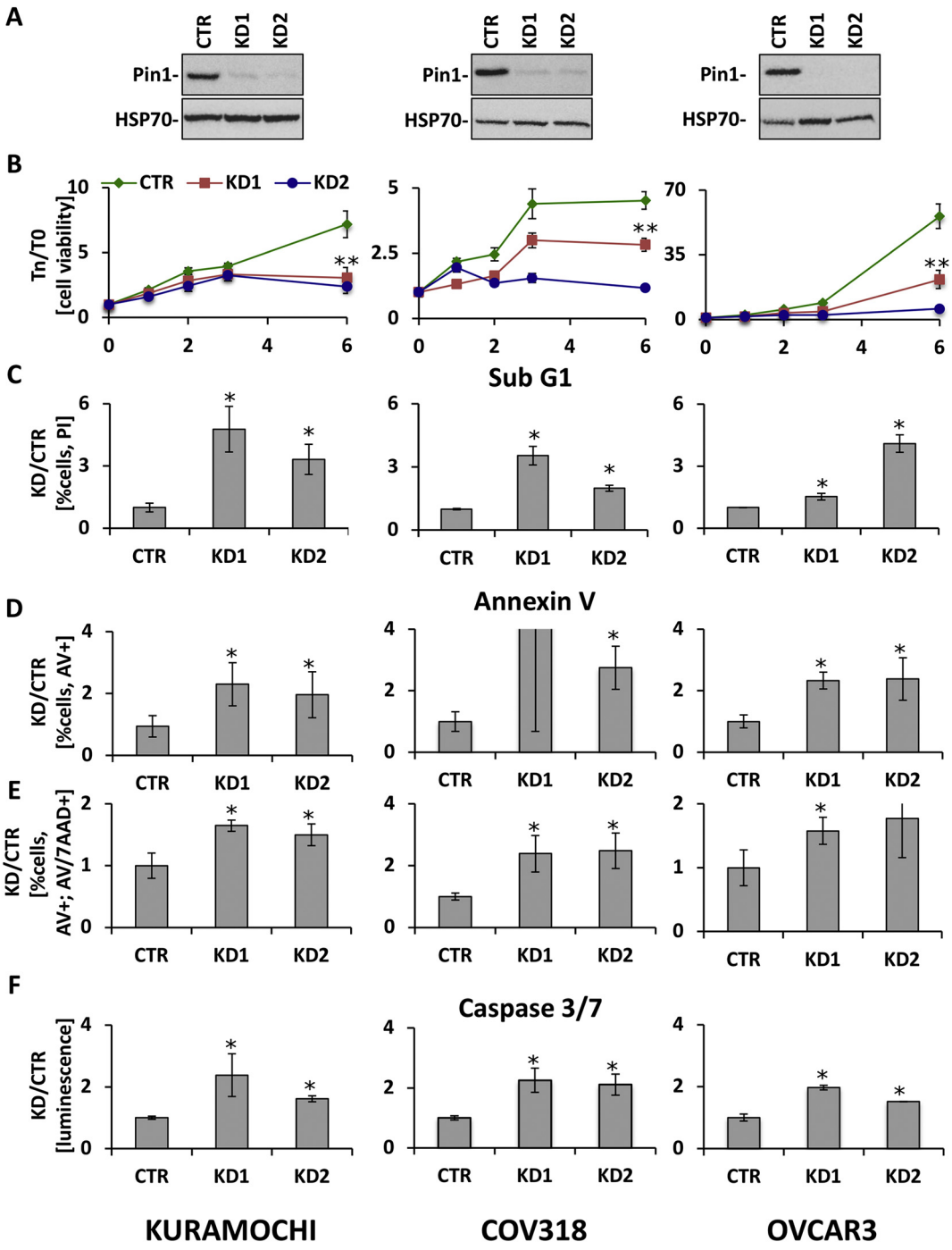


**Fig. 3.** Pin1 knock down induces apoptosis in ovarian cancer cell lines. Pin1 was KD in Kuramochi, COV318, and Ovcar3 cell lines. (A) Western blot analysis demonstrates the KD efficiency. (B) Cell viability was done in triplicates. X axis: days. (C) Sub G1 was determined by propidium iodide staining (≥ three independent experiments). (D) Early and (E) total apoptosis were determined by Annexin V/7-AAD staining (≥ three independent experiments). (F) Activation of caspase 3/7 was analyzed on cell extracts by luminescence assay (≥ two independent experiments). All the values on y-axis are normalized to the control. (*, $p$ value $< 0.05$).

### *3.5. LC8 promotes Pin1 protein degradation*

High affinity or covalent inhibitors promote degradation of Pin1 [36,65]. To assess the effect of LC8, fibroblast cells were treated with 100 μM of LC8. We observed that LC8 caused a decrease in the level of the Pin1 protein (Fig. 5A). At the mRNA level, the treatment did not substantially alter Pin1 (Fig. 5B). To discriminate between protein degradation or decreased stability, cells were treated with MG132 (proteasome inhibitor) (Fig. 5A) or CHX (protein synthesis inhibitor) (Fig. 5C). Only MG132 rescued the expression of Pin1 confirming a

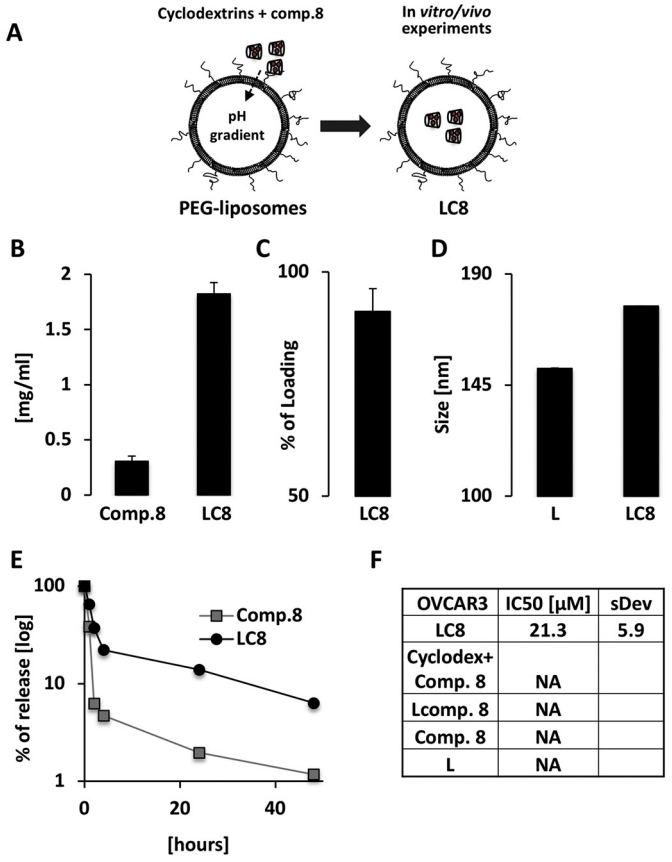


| OVCAR3 | IC50 [μM] | sDev |
|---|---|---|
| LC8 | 21.3 | 5.9 |
| Cyclodex+ Comp. 8 | NA | |
| Lcomp. 8 | NA | |
| Comp. 8 | NA | |
| L | NA | |

**Fig. 4.** LC8: chemico-physical properties and in vitro activity. (A) Schematic representation of the active loading of compound 8 (Comp.8) into pegylated liposomes. (B) LC8 increases the solubility of comp. 8 in PBS solution by about 6 times. (C) The loading efficiency of comp. 8 into pegylated liposomes is > 90%. (D) DLS analysis of liposomes before (L) and after loading of LC8.(E) Release of comp. 8 or LC8 through a semipermeable membrane. Representative result. (F) OVCAR3 cell line was treated with LC8, cyclodextrin/comp. 8, liposome/comp. 8, comp. 8, or empty liposomes (L) and the IC50 was determined after 96 h (NA: Not applicable).

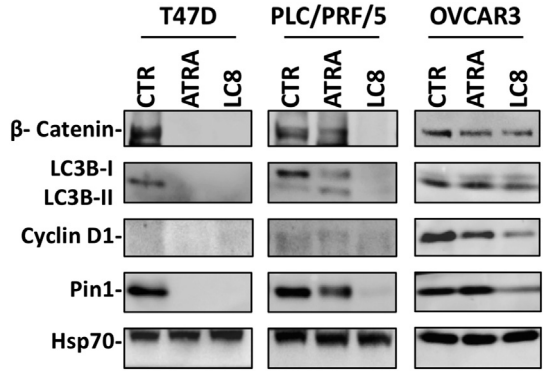


**Fig. 6.** LC8 alters the expression of Pin1 target proteins.T47D, PLC/PRF/5 and OVCAR3 cell lines were treated with 10 μM of ATRA (positive control) and 100 μM of LC8 for 24 h and analyzed by western blot. The expression of β-catenin, LC3B, and cyclin D1 was down regulated by LC8.

specific mechanism of protein degradation mediated by the proteasome.

### 3.6. LC8 alters the levels and function of PIN1 substrates

Pin1 controls multiple cancer drive-pathways through regulation of many oncogenes and tumor suppressor genes at various levels [27]. We utilized T47D (breast) and PLC/PRF/5 (liver) cancer cell lines as published models and OVCAR3 cell line to study LC8's effect [36,66]. Compared to untreated cells, LC8 downregulated the expression of ß-catenin, LC3B (autophagy), and cyclin D1 (cell cycle; only in OVCAR3 cells) (Fig. 6). As control we utilized ATRA, a recently published inhibitor of Pin1 [65], which provided similar results.

### 3.7. LC8 is a drug for HGSOC therapy

Liposomal drugs are mostly effective in vivo due to their designed formulation to accumulate inside the tumor (EPR effect) and increase drug solubility. Before testing the efficacy of LC8, we carried out a maximum tolerated dose (MTD) experiments. Mice were treated with a dose escalation of the liposomal formulation (without drug) and the health of the mice was monitored (body weight and histopathology analysis). We found that the mice could be treated up to 250 mg/kg

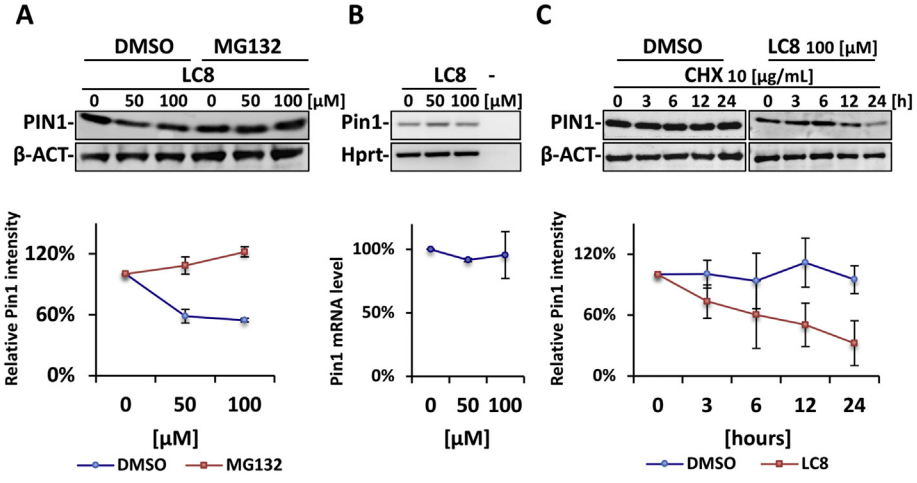


**Fig. 5.** LC8 induces Pin1 degradation through the proteasome. (A) Fibroblasts were treated with 100 μM of LC8 for 48 h followed by 10 μM of proteasomal inhibitor MG132 for 6 h. MG132 was able to rescue the expression of Pin1 protein. (B) Fibroblasts were treated as in (A). Pin1 RNA levels was unaffected. (C) Fibroblasts were treated with 100 μM of LC8 for 24 h followed by 10 μg/mL of CHX for the indicated time. LC8 induces protein degradation through the proteasome. Bottom panel: semiquantitative analysis was reported.

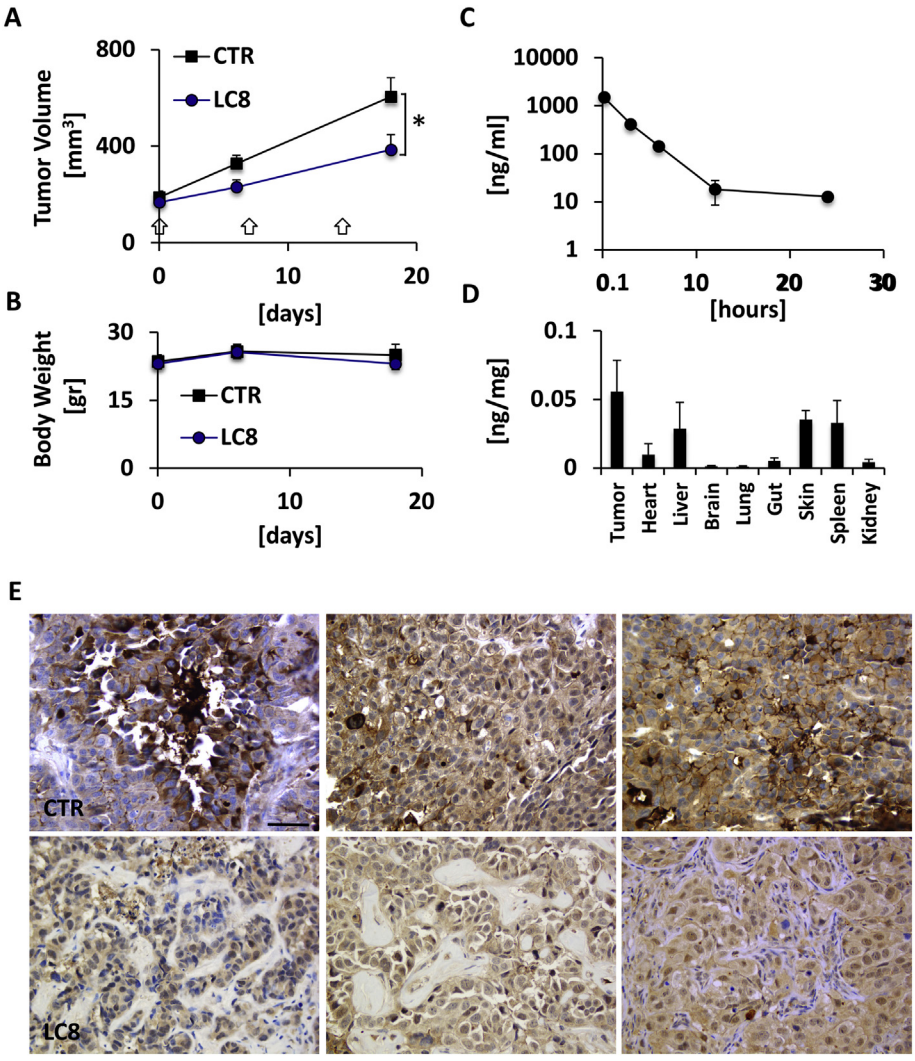


**Fig. 7.** LC8 is effective in a HGSOC mouse tumor model. Nude mice were subcutaneously injected with $5 \times 10^6$ OVCAR3 cell line (n = 12, group) and (A) tumor volume and (B) body weight were followed for 18 days. LC8 was injected i.p. every 7 days (arrows) at a dose of 20 mg/kg. LC8 was effective to reduce tumor burden without compromising animal health. (C) FVB/N mice (n = 3, data point) were i.p. injected with 20 mg/kg of LC8 and plasma was analyzed at indicated time point. Y axis: ng of drug/mL of blood (D) Nude mice (n = 3, data point) subcutaneously implanted with OVCAR3 cell line were i.p. injected with 20 mg/kg of LC8 and analyzed after 72 h. Y axis: ng of drug/mg of tissue. LC8 accumulated mainly in the tumor. (E) IHC evaluation of Pin1 expression in 3 tumors derived from (A and B). Scale bar: 100 μm.

without evident signs of toxicity (Fig. S3A,B). Afterwards, the mice were treated i.p. with LC8 at the indicated doses. As an objective scale of mouse health, the body weight was followed for almost 3 months. We observed no sign of toxicity up to 40 mg/kg (Fig. S4A,B).

OVCAR3 cells are a good model of HGSOC and can grow subcutaneously in nude mice. Cells were injected into the flank of the mice and after tumors reached a volume of 168 ± 28 $mm^3$, the animals were treated with 20 mg/kg of LC8 as in the MTD experiment. LC8 significantly decreased tumor volume compared to untreated mice (Fig. 7A). The body weight of the mice in both groups remained unchanged (Fig. 7B). Serum PK analysis of the drug showed two-kinetic phases of elimination, with a major decrement in the first 10 h (Fig. 7C). Interestingly, the biodistribution of LC8 after 72 h showed a main accumulation in the tumor followed by liver, spleen, and skin (Fig. 7D). Similar to Doxil[41], the liposomal formulation could avoid accumulation of doxorubicin in tissues with tight junctions and a well-developed lymphatic system such as in the heart. On the contrary, tumors with leaky vasculature and a poor lymphatic system allowed the accumulation of LC8, in turn increasing the efficacy of the drug. Although the circulation time of LC8 is far from Doxil, the volume of distribution is still low thus increasing the therapeutic index.

The effect of LC8 was evaluated on the expression of Pin1 in the tumors of mice treated with LC8 or untreated (PBS) as in Fig. 7A and B. LC8 downregulated the expression of Pin1 at background level (negative) as showed in Fig. 7E. In untreated mice, Pin1 has an intense cytoplasmic/nuclear staining.

## 4. Conclusions

This investigation is the first to report the preparation of an effective liposomal formulation of a potent and selective Pin1 inhibitor. The new nanoformulation improves the in vitro and in vivo pharmacological properties of the Pin1 inhibitor. We showed that Pin1 is overexpressed in human serous ovarian cancer and its inhibition induces cell death and tumor growth reduction in mouse metastatic immunocompetent ovarian and human subcutaneous ovarian cancer models. The development of such new active liposome formulations may pave the way for clinical experimentation and support for a new effective targeted therapy for ovarian cancer patients.

## Acknowledgments

Authors are grateful and would like to recognize the Associazione Italiana per la Ricerca sul Cancro – My First AIRC (n. 1569). Mrs. Laura Zannier and Antonella Selva for histopathology experiments.

## Competing interests

The authors declare no competing interests.

## References


[1] D.D. Bowtell, S. Böhm, A.A. Ahmed, P.-J. Aspuria, R.C. Bast, V. Beral, et al., Rethinking ovarian cancer II: reducing mortality from high-grade serous ovarian cancer, Nat. Rev. Cancer 15 (2015) 668–679.

[2] G.C. Jayson, E.C. Kohn, H.C. Kitchener, J.A. Ledermann, Ovarian cancer, Lancet 384 (2014) 1376–1388, http://dx.doi.org/10.1016/S0140-6736(13)62146-7.

[3] C. Della Pepa, G. Tonini, C. Pisano, M. Di Napoli, S.C. Cecere, R. Tambaro, et al., Ovarian cancer standard of care: are there real alternatives? Chin. J. Cancer 34 (2015) 17–27, http://dx.doi.org/10.5732/cjc.014.10274.

[4] B. Kaufman, R. Shapira-Frommer, R.K. Schmutzler, M.W. Audeh, M. Friedlander, J. Balmaña, et al., Olaparib monotherapy in patients with advanced Cancer and a germline *BRCA1/2*mutation, J. Clin. Oncol. 33 (2015) 244–250, http://dx.doi.org/10.1200/JCO.2014.56.2728.

[5] P.C. Fong, D.S. Boss, T.A. Yap, A. Tutt, P. Wu, M. Mergui-Roelvink, et al., Inhibition of poly(ADP-ribose) polymerase in tumors from *BRCA*mutation carriers, N. Engl. J. Med. 361 (2009) 123–134, http://dx.doi.org/10.1056/NEJMoa0900212.

[6] E. Pujade-Lauraine, F. Hilpert, B. Weber, A. Reuss, A. Poveda, G. Kristensen, et al., Bevacizumab combined with chemotherapy for platinum-resistant recurrent ovarian Cancer: the AURELIA open-label randomized phase III trial, J. Clin. Oncol. 32 (2014) 1302–1308, http://dx.doi.org/10.1200/JCO.2013.51.4489.

[7] C. Aghajanian, S.V. Blank, B.A. Goff, P.L. Judson, M.G. Teneriello, A. Husain, et al., OCEANS: a randomized, double-blind, placebo-controlled phase III trial of chemotherapy with or without bevacizumab in patients with platinum-sensitive recurrent epithelial ovarian, primary peritoneal, or fallopian tube cancer, J. Clin. Oncol. 30 (2012) 2039–2045, http://dx.doi.org/10.1200/JCO.2012.42.0505.

[8] T.J. Perren, A.M. Swart, J. Pfisterer, J.A. Ledermann, E. Pujade-Lauraine, G. Kristensen, et al., A phase 3 trial of bevacizumab in ovarian cancer, N. Engl. J. Med. 365 (2011) 2484–2496, http://dx.doi.org/10.1056/NEJMoa1103799.

[9] R.A. Burger, M.F. Brady, M.A. Bookman, G.F. Fleming, B.J. Monk, H. Huang, et al., Incorporation of bevacizumab in the primary treatment of ovarian Cancer, N. Engl. J. Med. 365 (2011) 2473–2483, http://dx.doi.org/10.1056/NEJMoa1104390.

[10] R. Perets, G.A. Wyant, K.W. Muto, J.G. Bijron, B.B. Poole, K.T. Chin, et al., Transformation of the fallopian tube secretory epithelium leads to high-grade serous ovarian cancer in Brca;Tp53;Pten models, Cancer Cell 24 (2013) 751–765, http://dx.doi.org/10.1016/j.ccr.2013.10.013.

[11] A. Flesken-Nikitin, C.-I. Hwang, C.-Y. Cheng, T.V. Michurina, G. Enikolopov, A.Y. Nikitin, Ovarian surface epithelium at the junction area contains a cancer-prone stem cell niche, Nature 495 (2013) 241–245, http://dx.doi.org/10.1038/nature11979.

[12] S. Vaughan, J.I. Coward, R.C. Bast, A. Berchuck, J.S. Berek, J.D. Brenton, et al., Rethinking ovarian cancer: recommendations for improving outcomes, Nat. Rev. Cancer 11 (2011) 719–725, http://dx.doi.org/10.1038/nrc3144.

[13] J. Kim, D.M. Coffey, C.J. Creighton, Z. Yu, S.M. Hawkins, M.M. Matzuk, High-grade serous ovarian cancer arises from fallopian tube in a mouse model, Proc. Natl. Acad. Sci. 109 (2012) 3921–3926, http://dx.doi.org/10.1073/pnas.1117135109.

[14] C.A. Sherman-Baust, E. Kuhn, B.L. Valle, I.-M. Shih, R.J. Kurman, T.-L. Wang, et al., A genetically engineered ovarian cancer mouse model based on fallopian tube transformation mimics human high-grade serous carcinoma development, J. Pathol. 233 (2014) 228–237, http://dx.doi.org/10.1002/path.4353.

[15] The Cancer Genome Atlas Research Network, Integrated genomic analyses of ovarian carcinoma, Nature 474 (2011) 609–615, http://dx.doi.org/10.1038/nature10166.

[16] H. Zhang, T. Liu, Z. Zhang, S.H. Payne, B. Zhang, J.E. McDermott, et al., Integrated Proteogenomic characterization of human high-grade serous ovarian Cancer, Cell 166 (2016) 755–765, http://dx.doi.org/10.1016/j.cell.2016.05.069.

[17] M.B. Yaffe, M. Schutkowski, M. Shen, X.Z. Zhou, P.T. Stukenberg, J.U. Rahfeld, et al., Sequence-specific and phosphorylation-dependent proline isomerization: a potential mitotic regulatory mechanism, Science 278 (1997) 1957–1960.

[18] R. Ranganathan, K.P. Lu, T. Hunter, J.P. Noel, Structural and functional analysis of the mitotic rotamase Pin1 suggests substrate recognition is phosphorylation dependent, Cell 89 (1997) 875–886.

[19] M. Gianni, A. Boldetti, V. Guarnaccia, A. Rambaldi, E. Parrella, I. Raska, et al., Inhibition of the peptidyl-prolyl-isomerase Pin1 enhances the responses of acute myeloid leukemia cells to retinoic acid via stabilization of RARalpha and PML-RARalpha, Cancer Res. 69 (2009) 1016–1026, http://dx.doi.org/10.1158/0008-5472.CAN-08-2603.

[20] J.E. Girardini, M. Napoli, S. Piazza, A. Rustighi, C. Marotta, E. Radaelli, et al., A Pin1/mutant p53 axis promotes aggressiveness in breast cancer, Cancer Cell 20 (2011) 79–91, http://dx.doi.org/10.1016/j.ccr.2011.06.004.

[21] P. Zacchi, M. Gostissa, T. Uchida, C. Salvagno, F. Avolio, S. Volinia, et al., The prolyl isomerase Pin1 reveals a mechanism to control p53 functions after genotoxic insults, Nature 419 (2002) 853–857, http://dx.doi.org/10.1038/nature01120.

[22] R. La Montagna, I. Caligiuri, P. Maranta, C. Lucchetti, L. Esposito, M.G. Paggi, et al., Androgen receptor serine 81 mediates Pin1 interaction and activity, Cell Cycle 11 (2012) 3415–3420.

[23] F. Rizzolio, C. Lucchetti, I. Caligiuri, I. Marchesi, M. Caputo, A.J. Klein-Szanto, et al., Retinoblastoma tumor-suppressor protein phosphorylation and inactivation depend on direct interaction with Pin1, Cell Death Differ. 19 (2012) 1152–1161, http://dx.doi.org/10.1038/cdd.2011.202.

[24] C. Lucchetti, I. Caligiuri, G. Toffoli, A. Giordano, F. Rizzolio, The prolyl isomerase Pin1 acts synergistically with CDK2 to regulate the basal activity of estrogen receptor α in breast Cancer, PLoS One 8 (2013) e55355, , http://dx.doi.org/10.1371/journal.pone.0055355.

[25] R. La Montagna, I. Caligiuri, A. Giordano, F. Rizzolio, Pin1 and nuclear receptors: a new language? J. Cell. Physiol. 228 (2013) 1799–1801, http://dx.doi.org/10.1002/jcp.24316.

[26] F. Rizzolio, I. Caligiuri, C. Lucchetti, R. Fratamico, V. Tomei, G. Gallo, et al., Dissecting Pin1 and phospho-pRb regulation, J. Cell. Physiol. 228 (2013) 73–77, http://dx.doi.org/10.1002/jcp.24107.

[27] X.Z. Zhou, K.P. Lu, The isomerase PIN1 controls numerous cancer-driving pathways and is a unique drug target, Nat. Rev. Cancer 16 (2016) 463–478, http://dx.doi.org/10.1038/nrc.2016.49.

[28] J.D. Moore, A. Potter, Pin1 inhibitors: pitfalls, progress and cellular pharmacology, Bioorg. Med. Chem. Lett. 23 (2013) 4283–4291, http://dx.doi.org/10.1016/j.bmcl.2013.05.088.

[29] Y.C. Liou, A. Ryo, H.K. Huang, P.J. Lu, R. Bronson, F. Fujimori, et al., Loss of Pin1 function in the mouse causes phenotypes resembling cyclin D1-null phenotypes, Proc. Natl. Acad. Sci. U. S. A. 99 (2002) 1335–1340, http://dx.doi.org/10.1073/pnas.032404099032404099.

[30] Z. Lu, T. Hunter, Prolyl isomerase Pin1 in cancer, Cell Res. 24 (2014) 1033–1049, http://dx.doi.org/10.1038/cr.2014.109.

[31] A. Singh, J. Settleman, EMT, cancer stem cells and drug resistance: an emerging axis of evil in the war on cancer, Oncogene 29 (2010) 4741–4751, http://dx.doi.org/10.1038/onc.2010.215.

[32] A. Rustighi, A. Zannini, L. Tiberi, R. Sommaggio, S. Piazza, G. Sorrentino, et al., Prolyl-isomerase Pin1 controls normal and cancer stem cells of the breast, EMBO Mol. Med. 6 (2014) 99–119, http://dx.doi.org/10.1002/emmm.201302909.

[33] Q. Ding, L. Huo, J.-Y. Yang, W. Xia, Y. Wei, Y. Liao, et al., Down-regulation of myeloid cell Leukemia-1 through inhibiting Erk/pin 1 pathway by Sorafenib facilitates Chemosensitization in breast Cancer, Cancer Res. 68 (2008) 6109–6117, http://dx.doi.org/10.1158/0008-5472.CAN-08-0579.

[34] C. Guo, X. Hou, L. Dong, J. Marakovits, S. Greasley, E. Dagostino, et al., Structure-based design of novel human Pin1 inhibitors (III): optimizing affinity beyond the phosphate recognition pocket, Bioorg. Med. Chem. Lett. 24 (2014) 4187–4191, http://dx.doi.org/10.1016/j.bmcl.2014.07.044.

[35] I. Palmero, A.J. Sinclair, G. Peters, P.J. Farrell, EBNA-2 and EBNA-LP cooperate to cause G0 to G1 transition during immortalization of resting human B lymphocytes by Epstein-Barr virus, EMBO J. 13 (1994).

[36] E. Campaner, A. Rustighi, A. Zannini, A. Cristiani, S. Piazza, Y. Ciani, et al., A covalent PIN1 inhibitor selectively targets cancer cells by a dual mechanism of action, Nat. Commun. 8 (2017) 15772, , http://dx.doi.org/10.1038/ncomms15772.

[37] E. Blanco, H. Shen, M. Ferrari, Principles of nanoparticle design for overcoming biological barriers to drug delivery, Nat. Biotechnol. 33 (2015) 941–951, http://dx.doi.org/10.1038/nbt.3330.

[38] Y. Matsumura, H. Maeda, A new concept for macromolecular therapeutics in cancer chemotherapy: mechanism of tumoritropic accumulation of proteins and the antitumor agent smancs, Cancer Res. 46 (1986) 6387–6392.

[39] K. Greish, Enhanced permeability and retention (EPR) effect for anticancer nanomedicine drug targeting, Methods Mol. Biol. (2010) 25–37, http://dx.doi.org/10.1007/978-1-60761-609-2_3.

[40] S. Palazzolo, S. Bayda, M. Hadla, I. Caligiuri, G. Corona, G. Toffoli, et al., The clinical translation of organic nanomaterials for Cancer therapy: afocus on polymeric nanoparticles, micelles, liposomes and exosomes, Curr. Med. Chem. 24 (2017), http://dx.doi.org/10.2174/0929867324666170830113755.

[41] S. Bayda, M. Hadla, G. Corona, G. Toffoli, F. Rizzolio, F. Rizzolio, Inorganic nanoparticles for Cancer therapy: a transition from lab to clinic, Curr. Med. Chem. 25 (2017), http://dx.doi.org/10.2174/0929867325666171229141156.

[42] Y. Barenholz, Doxil®–the first FDA-approved nano-drug: lessons learned, J. Control. Release 160 (2012) 117–134, http://dx.doi.org/10.1016/j.jconrel.2012.03.020.

[43] E. Miele, G.P. Spinelli, E. Miele, F. Tomao, S. Tomao, Albumin-bound formulation of paclitaxel (Abraxane ABI-007) in the treatment of breast cancer, Int. J. Nanomedicine 4 (2009) 99–105.

[44] U. Bulbake, S. Doppalapudi, N. Kommineni, W. Khan, Liposomal formulations in clinical use: an updated review, Pharmaceutics 9 (2017) 12, http://dx.doi.org/10.3390/pharmaceutics9020012.

[45] D. Bobo, K.J. Robinson, J. Islam, K.J. Thurecht, S.R. Corrie, Nanoparticle-based medicines: areview of FDA-approved materials and clinical trials to date, Pharm. Res. 33 (2016) 2373–2387, http://dx.doi.org/10.1007/s11095-016-1958-5.

[46] S. Sur, A.C. Fries, K.W. Kinzler, S. Zhou, B. Vogelstein, Remote loading of preencapsulated drugs into stealth liposomes, Proc. Natl. Acad. Sci. 111 (2014) 2283–2288, http://dx.doi.org/10.1073/pnas.1324135111.

[47] M. Napoli, J.E. Girardini, S. Piazza, G. Del Sal, Wiring the oncogenic circuitry: Pin1 unleashes mutant p53, Oncotarget 2 (2011) 654–656 (doi:329).

[48] G. Ayala, D. Wang, G. Wulf, A. Frolov, R. Li, J. Sowadski, et al., The prolyl isomerase Pin1 is a novel prognostic marker in human prostate cancer, Cancer Res. 63 (2003) 6244–6251.

[49] P.B. Lam, L.N. Burga, B.P. Wu, E.W. Hofstatter, K.P. Lu, G.M. Wulf, Prolyl isomerase Pin1 is highly expressed in Her2-positive breast cancer and regulates erbB2 protein

stability, Mol. Cancer 7 (2008) 91, http://dx.doi.org/10.1186/1476-4598-7-91.
[50] K.-W. Leung, C.-H. Tsai, M. Hsiao, C.-J. Tseng, L.-P. Ger, K.-H. Lee, et al., Pin1 overexpression is associated with poor differentiation and survival in oral squamous cell carcinoma, Oncol. Rep. 21 (2009) 1097–1104.
[51] P. Jawanjal, S. Salhan, I. Dhawan, R. Tripathi, G. Rath, Peptidyl-prolyl isomerase Pin1-mediated abrogation of APC-β-catenin interaction in squamous cell carcinoma of cervix, Romanian J. Morphol. Embryol. 55 (2014) 83–90.
[52] C.-X. Zhou, Y. Gao, Aberrant expression of beta-catenin, Pin1 and cylin D1 in salivary adenoid cystic carcinoma: relation to tumor proliferation and metastasis, Oncol. Rep. 16 (2006) 505–511.
[53] F.-C. Lin, Y.-C. Lee, Y.-G. Goan, C.-H. Tsai, Y.-C. Yao, H.-C. Cheng, et al., Pin1 positively affects tumorigenesis of esophageal squamous cell carcinoma and correlates with poor survival of patients, J. Biomed. Sci. 21 (2014) 75, , http://dx.doi.org/10.1186/s12929-014-0075-1.
[54] J. Kuramochi, T. Arai, S. Ikeda, J. Kumagai, H. Uetake, K. Sugihara, High Pin1 expression is associated with tumor progression in colorectal cancer, J. Surg. Oncol. 94 (2006) 155–160, http://dx.doi.org/10.1002/jso.20510.
[55] L. Bao, A. Kimzey, G. Sauter, J.M. Sowadski, K.P. Lu, D.G. Wang, Prevalent overexpression of prolyl isomerase Pin1 in human cancers, Am. J. Pathol. 164 (2004) 1727–1737.
[56] S. Domcke, R. Sinha, D.A. Levine, C. Sander, N. Schultz, Evaluating cell lines as tumour models by comparison of genomic profiles, Nat. Commun. 4 (2013) 2126, , http://dx.doi.org/10.1038/ncomms3126.
[57] K.L. Thu, M. Papari-Zareei, V. Stastny, K. Song, M. Peyton, V.D. Martinez, et al., A comprehensively characterized cell line panel highly representative of clinical ovarian high-grade serous carcinomas, Oncotarget 8 (2017) 50489–50499, http://dx.doi.org/10.18632/oncotarget.9929.
[58] A.K. Mitra, D.A. Davis, S. Tomar, L. Roy, H. Gurler, J. Xie, et al., In vivo tumor growth of high-grade serous ovarian cancer cell lines, Gynecol. Oncol. 138 (2015) 372–377, http://dx.doi.org/10.1016/j.ygyno.2015.05.040.
[59] C.W. McCloskey, R.L. Goldberg, L.E. Carter, L.F. Gamwell, E.M. Al-Hujaily, O. Collins, et al., A new spontaneously transformed syngeneic model of high-grade serous ovarian cancer with a tumor-initiating cell population, Front. Oncol. 4 (2014) 53, , http://dx.doi.org/10.3389/fonc.2014.00053.
[60] H.-I. Chang, M.-K. Yeh, Clinical development of liposome-based drugs: formulation, characterization, and therapeutic efficacy, Int. J. Nanomed. 7 (2012) 49–60, http://dx.doi.org/10.2147/IJN.S26766.
[61] A. Gabizon, H. Shmeeda, Y. Barenholz, Pharmacokinetics of pegylated liposomal doxorubicin: review of animal and human studies, Clin. Pharmacokinet. 42 (2003) 419–436, http://dx.doi.org/10.2165/00003088-200342050-00002.
[62] J. Gubernator, Active methods of drug loading into liposomes: recent strategies for stable drug entrapment and increased *in vivo* activity, Expert Opin. Drug Deliv. 8 (2011) 565–580, http://dx.doi.org/10.1517/17425247.2011.566552.
[63] L. Dong, J. Marakovits, X. Hou, C. Guo, S. Greasley, E. Dagostino, et al., Structure-based design of novel human Pin1 inhibitors (II), Bioorg. Med. Chem. Lett. 20 (2010) 2210–2214, http://dx.doi.org/10.1016/j.bmcl.2010.02.033.
[64] C. Guo, X. Hou, L. Dong, E. Dagostino, S. Greasley, R. Ferre, et al., Structure-based design of novel human Pin1 inhibitors (I), Bioorg. Med. Chem. Lett. 19 (2009) 5613–5616, http://dx.doi.org/10.1016/j.bmcl.2009.08.034.
[65] S. Wei, S. Kozono, L. Kats, M. Nechama, W. Li, J. Guarnerio, et al., Active Pin1 is a key target of all-trans retinoic acid in acute promyelocytic leukemia and breast cancer, Nat. Med. 21 (2015) 457–466, http://dx.doi.org/10.1038/nm.3839.
[66] X.-H. Liao, A.L. Zhang, M. Zheng, M.-Q. Li, C.P. Chen, H. Xu, et al., Chemical or genetic Pin1 inhibition exerts potent anticancer activity against hepatocellular carcinoma by blocking multiple cancer-driving pathways, Sci. Rep. 7 (2017) 43639, , http://dx.doi.org/10.1038/srep43639.